



Published in final edited form as:

*Immunol Cell Biol.* 2014 July ; 92(6): 499–508. doi:10.1038/icb.2014.13.

## CX<sub>3</sub>CR1 Delineates Temporally and Functionally Distinct Subsets of Myeloid-Derived Suppressor Cells in a Mouse Model of Ovarian Cancer

Kevin M. Hart<sup>1</sup>, Edward J. Usherwood<sup>1</sup>, and Brent L. Berwin<sup>1</sup>

<sup>1</sup>Department of Microbiology and Immunology, Dartmouth Medical Center, Lebanon NH 03756

### Abstract

Expression of the chemokine receptor CX<sub>3</sub>CR1 has been used to identify distinct populations within the monocyte, macrophage and dendritic cell lineages. Recent evidence indicates that CX<sub>3</sub>CR1-positive subsets of myeloid cells play distinct and important roles in a wide range of immunological maladies and thus the use of CX<sub>3</sub>CR1 expression has leveraged our understanding of the myeloid contribution to a multitude of diseases. Here we use CX<sub>3</sub>CR1 expression as a means to identify a novel non-granulocytic CX<sub>3</sub>CR1-negative myeloid population that is functionally distinct from the previously-described CX<sub>3</sub>CR1-positive cellular subsets within the CD11b-positive cellular compartment of ascites from ovarian tumor-bearing mice. We functionally identify CX<sub>3</sub>CR1-negative cells as myeloid suppressor cells and as a cellular subset with pathological specificity. Importantly, the CX<sub>3</sub>CR1-negative cells exhibit early IL-10 production in the ovarian tumor microenvironment, which we have shown to be critically tied to suppression and further MDSC accumulation, and we now show that this cellular population actively contributes to tumor progression. Furthermore, we demonstrate that the CX<sub>3</sub>CR1-negative population is derived from the recently described CX<sub>3</sub>CR1-positive macrophage/dendritic cell precursor (MDP) cell. These studies provide a greater understanding of the generation and maintenance of regulatory myeloid subsets and have broad implications for the elucidation of myeloid function and contributions within the tumor microenvironment.

### Keywords

myeloid; ovarian cancer; immunosuppression

### Introduction

Expression of the chemokine receptor CX<sub>3</sub>CR1 is a hallmark of committed macrophage/dendritic cell precursors (MDP) and variable expression of CX<sub>3</sub>CR1 has recently been used to identify distinct populations within the monocyte, macrophage and dendritic cell lineages. In mice, blood monocytes have been divided into two populations based on high and low

Users may view, print, copy, and download text and data-mine the content in such documents, for the purposes of academic research, subject always to the full Conditions of use:[http://www.nature.com/authors/editorial\\_policies/license.html#terms](http://www.nature.com/authors/editorial_policies/license.html#terms)

### Authorship

K.H. and B.B. both contributed to the study's conception, design and execution. E.J.U. contributed reagents and advice.

expression of CX<sub>3</sub>CR1 relative to one another. These two subsets can also be identified in the blood by the differential expression of the Ly6C antigen of GR-1, CD62L and CCR2<sup>1, 2</sup>. Accumulating evidence indicates that CX<sub>3</sub>CR1-positive myeloid cells play an important role in a wide range of immunological maladies including colitis<sup>3, 4</sup>, burn healing<sup>5</sup>, pulmonary vaccinia infection<sup>6</sup>, CNS injury<sup>7</sup>, liver fibrosis<sup>8</sup>, ovarian cancer<sup>9</sup>, diabetes<sup>10</sup> and obesity<sup>10, 11</sup>. Moreover, in different contexts the CX<sub>3</sub>CR1-positive cells can be immunostimulatory (protection in a vaccinia lung infection model<sup>6</sup> and drive bactericidal defenses during septic peritonitis<sup>12</sup>) but can also be immuno-regulatory including inhibition of T cell mediated colitis<sup>3</sup>, accumulation of TGF-beta producing macrophages in wounds<sup>13</sup>, and limiting airway hyperresponsiveness<sup>14</sup>.

We recently employed CX<sub>3</sub>CR1-GFP reporter mice to characterize the tumor-infiltrating myeloid cells in the ID8vβ murine model of ovarian cancer. From these studies we observed a progressive accumulation of CX<sub>3</sub>CR1-positive myeloid cells during tumor progression in the tumor microenvironment<sup>9</sup>. Amongst the CX<sub>3</sub>CR1<sup>+</sup> cell subsets we identified that early tumor development is marked by the presence of infiltrating CX<sub>3</sub>CR1<sup>+</sup>GR-1<sup>-</sup> positive cells, but is progressively dominated by a population of suppressive CX<sub>3</sub>CR1<sup>+</sup>GR-1<sup>lo</sup> cells, which express CD11b, CD115, and variable levels of F4/80 and CD11c; the loss of GR-1 expression on the CX<sub>3</sub>CR1-positive cells seen later in tumor progression seems to be a consequence of entering the peritoneum rather than preferential recruitment of a specific monocyte subset<sup>9</sup>. Importantly, both subsets of CX<sub>3</sub>CR1<sup>+</sup> cells were identified to function as myeloid-derived suppressor cells (MDSC) within the ovarian tumor microenvironment. Accumulated evidence from our lab and others has clearly demonstrated that MDSCs within the ovarian tumor microenvironment are critical to ovarian cancer progression<sup>9, 15–18</sup> and, specifically, that MDSC-derived IL-10 plays a crucial role in sculpting the microenvironment. IL-10 is both produced by, and acts upon, the bulk non-granulocytic CD11b-positive myeloid compartment in the ascites<sup>19–21</sup> and is intricately tied to clinical tumor progression<sup>22–24</sup>. Notably, the IL-10<sup>-</sup>expressing MDSCs enforce the suppressive tumor micro-environment, are potently inhibitory to T cell activity, and accumulation of the MDSCs, characterized to date as CX<sub>3</sub>CR1-positive, over the course of tumor progression favors tumor growth. Thus, use of CX<sub>3</sub>CR1 expression to distinguish subpopulations of tumor-infiltrating myeloid cells provides a powerful mechanism to dissect the phenotypic and functional changes in the myeloid compartment that occur during tumor progression.

We now report a population of CX<sub>3</sub>CR1-negative MDSCs within the ovarian tumor microenvironment that are temporally and functionally distinct from the CX<sub>3</sub>CR1-positive cells. With the use of a novel combination of CX<sub>3</sub>CR1 and IL-10 reporter mice we have identified a population of CX<sub>3</sub>CR1-negative MDSCs which express F4/80 and CD11b and are functionally immunosuppressive. Furthermore, we demonstrate that this CX<sub>3</sub>CR1-negative population is derived from the recently described CX<sub>3</sub>CR1-positive macrophage/dendritic cell precursor (MDP). Temporally, the CX<sub>3</sub>CR1-negative and CX<sub>3</sub>CR1-positive cells exhibit sequential IL-10 production over the course of tumor progression, which suggests that the CX<sub>3</sub>CR1-negative cells are critical for the initiation and generation of the tumor microenvironment and may influence the phenotype and function of subsequent infiltrating myeloid cells. Importantly, a novel cellular depletion method based on IL-10 expression reveals that the early IL-10-producing cells, dominated by CX<sub>3</sub>CR1-negative

MDSC, functionally contribute to tumor progression. These studies provide a greater understanding of the generation and maintenance of regulatory myeloid subsets and have broad implications for myeloid function.

## Methods

### Mice

Female C57BL/6 mice (*Mus musculus*) were purchased from the National Cancer Institute (Fredericksburg, MD USA). CX<sub>3</sub>CR1-GFP<sup>25</sup> mice were purchased from Jackson Laboratories (Bar Harbor, ME USA). IL-10BiT reporter mice<sup>26</sup> used in collaboration with Edward Usherwood (Dartmouth Medical School) were bred with CX<sub>3</sub>CR1-GFP mice to obtain CX<sub>3</sub>CR1/IL-10BiT double transgenic reporters. All animal experiments were approved by the Dartmouth Medical School Institutional Animal Care and Use Committee.

### Cells and Antibodies

ID8 cells transduced with Vegf-A and  $\beta$ Def29 (referred to as ID8v $\beta$  within this manuscript) were generated and maintained as previously described<sup>27</sup>. Anti-mouse Fc Block (San Jose, CA USA). Anti-mouse CD3 (145-2C11), Gr-1 (RB6-8C5), CD11b (M1/70), CD45.1 (A20), and Ly6C (HK1.4) were purchased from eBioscience (San Diego, CA USA). Anti-mouse Thy1.1 (OX-7), CD11c (N418), NK1.1 (PK136), CD115 (AFS98), F4/80 (BM8), Ly6G (1A8), CD45.2 (104), and BCL-2 (BCL/10C4) were purchased from Biolegend (San Diego, CA USA).

### Tumors and Leukocyte Isolation

Ovarian tumors were generated by i.p. injection of  $5 \times 10^6$  ID8v $\beta$  cells as previously described<sup>27</sup>. At the indicated time points ascites and blood were harvested from mice and the cellular fraction was collected. Additionally, peritoneal cells from naïve animals were collected by three 5 mL lavages with ice cold PBS. Single cell suspensions from bone marrow isolated from femurs and were obtained by passing tissues through a 70 $\mu$ m cell strainer (BD Biosciences, San Jose CA USA). Single cell suspensions were treated with ACK lysis buffer (0.15 M NH<sub>4</sub>Cl, 1.0 mM KHCO<sub>3</sub>, 0.1 mM EDTA) to remove red blood cells. Cells were resuspended in 0.5% BSA in PBS or media for further analysis or sorting. For bone marrow cultures, whole bone marrow was seeded at  $1 \times 10^6$  cells per well in a 48 well plate, cells were cultured overnight in complete medium, stimulated for 24 hours the following day with 20% plasma isolated from tumor ascites and analyzed by FACS.

### Fluorescence Activated Cell Sorting

Cells from mouse ID8v $\beta$  ascites, bone marrow from femurs, and blood were incubated with Fc blocking antibody (clone 2.4G2) prior to staining with the indicated primary antibodies. Flow Cytometry and cell sorting was done on the Accuri C6 and BD FACSAria (BD Biosciences, San Jose, CA USA). Flow data was analyzed using CFlow (BD Biosciences, San Jose, CA USA) and FlowJo 8.8.2 software (Treestar Inc, Ashland, OR USA).

## Chimeric Mice

For MDP chimeric mouse studies similar methods as described by Fogg et al. were employed. Briefly, bone marrow was collected from femurs, treated with red blood cell lysis buffer, washed and resuspended in PBS. Sorted Ly5.1 (CD45.1) MDP (CX<sub>3</sub>CR1-GFP lin-negative (CD11b, CD11c, CD3, GR-1, NK1.1, B220) ( $2 \times 10^4$  MDP, purity 90%) were admixed with  $1 \times 10^6$  whole C57BL/6 bone marrow. Mixed bone marrow was injected intravenously by para-orbital injection into irradiated (approximately 1000 rads) naïve C57BL/6 recipients.

## Immunosuppression Assays and IL-10 ELISA

Sorted CX<sub>3</sub>CR1 cell populations from naïve and tumor bearing mice (purity 90%) were co-cultured at the indicated ratios with  $10^6$  naïve splenocytes. Plated splenocytes were stimulated with 1 µg anti-CD3 (145-2C11) (BioXCell, West Lebanon, NH USA) and culture supernatants were collected after 72 hours and analyzed for IFN- $\gamma$  production using murine DuoSet ELISA (R&D Systems, Minneapolis, MN USA). Additionally, sorted populations were plated at  $1.5\text{--}3 \times 10^6$  cells per well with or without 100 ng/ml LPS stimulation (Sigma Aldrich, St. Louis, MO) and cultured for 72 hours. Supernatants were assessed for IL-10 production per  $10^5$  cells using a murine DuoSet ELISA (R&D Systems, Minneapolis, MN USA).

## Therapeutic Depletion of IL-10 –Expressing Cells

IL-10 reporter positive cells were depleted in tumor-bearing IL-10BiT mice through intraperitoneal injection of anti-Thy1.1 antibody (500 µg), provided by Edward Usherwood (Dartmouth Medical School, Lebanon, NH, USA), on days 7 and 10 post tumor injection. Mice were sacrificed on days 11 and 15 to assess peritoneal cell numbers and composition by flow cytometry. Additional mice were monitored and sacrificed when they became moribund. Statistical analysis of survival was determined by Kaplan–Meier analysis.

## Statistical analyses

All data were analyzed with Prism (GraphPad Software). Data were considered significant for *P* values less than 0.05 when performing a two-tailed *t*-test or Kaplan–Meier analysis. Differences are noted as \*  $p < 0.05$ , \*\*  $p < 0.01$ , \*\*\*  $p < 0.001$ . Sample sizes for each experiment are noted in the text. Values are shown as means  $\pm$  standard deviation.

## Results

### The non-granulocytic CD11b compartment in the tumor microenvironment is comprised of CX<sub>3</sub>CR1-positive and CX<sub>3</sub>CR1-negative myeloid populations

Our previous work and other reports indicate that resident peritoneal macrophages are CX<sub>3</sub>CR1-negative, while monocytes and MDSC recruited in inflammation and ovarian cancer are CX<sub>3</sub>CR1-positive<sup>2, 9</sup>. We recently identified a population of tumor-infiltrating CD11b<sup>+</sup>, IL-10 –producing, myeloid cells in the ascites to be critically tied to ovarian tumor progression through enforcement of a suppressive tumor microenvironment that included both the CX<sub>3</sub>CR1-positive and negative subsets<sup>19</sup>. Therefore, we undertook phenotypic and

functional analyses of the CX<sub>3</sub>CR1-positive and negative populations in the peritoneum of naïve and tumor-bearing mice to further clarify the lineage and contributions of the two populations, particularly in regard to the poorly-described CX<sub>3</sub>CR1-negative cells.

When we compared naïve and tumor-bearing CX<sub>3</sub>CR1-GFP reporter mice to wild-type tumor bearing mice, we observed that in the tumor microenvironment CX<sub>3</sub>CR1 expression divides the bulk CD11b-positive cells into two populations of CD11b-positive, CSF-1 receptor-positive, and Ly6C-low cells (Fig. 1a). Within a naïve peritoneal lavage, the population of CX<sub>3</sub>CR1-negative resident macrophages represents approximately two-thirds of the cells, whereas in the ascites it accounts for only a tenth of the total cells. Additionally, the CX<sub>3</sub>CR1-negative population expressed slightly higher levels of F4/80 compared to the CX<sub>3</sub>CR1-positive cells in the naïve peritoneum, although less dramatically in the tumor peritoneum, and was notably negative for Ly6G (Supplementary Fig. 1). Parallel analyses of wild-type mice lacking the CX<sub>3</sub>CR1-GFP transgene confirmed that the CX<sub>3</sub>CR1-low cells are indeed CX<sub>3</sub>CR1-negative (Fig. 1A). Thus, CX<sub>3</sub>CR1-GFP expression denotes two distinct populations within the tumor that share similar expression of other common myeloid markers.

Since the CX<sub>3</sub>CR1-negative population identified here is part of the larger CD11b compartment that we previously studied with T cell suppressive activity<sup>9</sup>, we next interrogated the specific suppressive capability of the CX<sub>3</sub>CR1-negative cells. We sorted CX<sub>3</sub>CR1-negative and -positive populations from tumor-bearing mice and titrated them into a mixed splenocyte reaction. Notably, the CX<sub>3</sub>CR1-negative population was functionally as suppressive as the CX<sub>3</sub>CR1-positive population, which we had previously demonstrated to be robustly suppressive in this assay (Fig. 1B). To assess the relative functional contribution of the two populations to the overall tumor microenvironment, we calculated total numbers of each within the peritoneum over the course of tumor progression. The total numbers of CX<sub>3</sub>CR1-negative cells increased during tumor progression, though in fewer total numbers of cells than the CX<sub>3</sub>CR1-positive cells (Fig. 1C). These studies demonstrate that the CX<sub>3</sub>CR1-negative fraction in the CD11b compartment is a critical component of the suppressive population of myeloid cells in the tumor. Importantly, by functional activity, this now identifies a CX<sub>3</sub>CR1-negative MDSC population in addition to the previously described CX<sub>3</sub>CR1-positive MDSC population.

### **IL-10 is produced within the ovarian tumor microenvironment by two distinct myeloid populations as assessed with the use of CX<sub>3</sub>CR1-GFP/IL-10BiT reporter mice**

Our previous description of CX<sub>3</sub>CR1 expression as a means to identify and track tumor-infiltrating MDSC in syngeneic ID8- VEGF-A/βDEF29 (ID8vβ) murine ovarian tumors allows us to specifically measure the molecular and cellular contribution of this subset of CD11b-positive cells to tumor progression<sup>9</sup>. To determine the extent that cellular subsets contribute to tumor supportive IL-10 production we generated CX<sub>3</sub>CR1-GFP/IL-10BiT dual reporter mice by crossing CX<sub>3</sub>CR1-GFP mice<sup>25</sup> with IL-10BiT reporter mice<sup>26</sup>. These mice permit us to assess the CX<sub>3</sub>CR1-delineated cellular subsets within the ID8vβ ascites for IL-10 production within the tumor microenvironment. In our previous analyses<sup>9</sup> we discerned the previously-described CX<sub>3</sub>CR1 -hi and -lo subsets of myeloid cells<sup>2</sup> in the

ascites by relative GFP expression, but due to a lack of detectable differences in function and phenotype distinguishing these cells in the ascites, we will refer to them collectively as CX<sub>3</sub>CR1-positive cells in these studies.

Analyses of advanced ascites from the CX<sub>3</sub>CR1-GFP/IL-10BiT tumor-bearing mice revealed IL-10 production from both the CX<sub>3</sub>CR1-positive and -negative populations of cells (Figs. 2A and B). Approximately one quarter of the CX<sub>3</sub>CR1-positive cells and ten percent of the CX<sub>3</sub>CR1-negative population were IL-10 reporter-positive when compared to the negative control of cells derived from a CX<sub>3</sub>CR1-GFP mouse lacking the IL-10BiT reporter (Fig. 2B). The IL-10 -producing cells from the CX<sub>3</sub>CR1-positive population represented approximately 7.5 percent of the cells in the ascites, while the IL-10 producing cells from the CX<sub>3</sub>CR1-negative population represented a smaller 2.5 percent (Fig. 2C). In order to confirm the reporter staining, we sorted CX<sub>3</sub>CR1-negative or positive cells from the CD11b-positive compartment in the ascites of tumor bearing mice. The sorted cells were cultured with or without LPS stimulation for 72 hours and IL-10 production in the supernatants was assessed by ELISA. We detected equivalent production of IL-10 per 10<sup>5</sup> cells from both populations, demonstrating that both populations are producing IL-10 directly *ex vivo* (Fig. 2D). Thus, positive and negative CX<sub>3</sub>CR1 expression delineates two distinct populations of IL-10-producing cells within the CD11b compartment in the tumor microenvironment. Importantly, this reveals that the CX<sub>3</sub>CR1-negative population contributes to IL-10 expression within the tumor microenvironment.

### Differential temporal contributions of IL-10 production in the tumor microenvironment by distinct MDSC subsets

In light of our previous findings in murine models of ovarian cancer that IL-10 signaling drives myeloid suppression, the contribution of the CX<sub>3</sub>CR1-negative population to IL-10 in the tumor microenvironment suggests a role in the development and maintenance of suppression within the tumor. Thus, we next endeavored to define the relationship of this population to CX<sub>3</sub>CR1-positive monocytes and MDSC, which have previously been described to be critical to the IL-10 network<sup>19</sup>.

We used the CX<sub>3</sub>CR1-GFP/IL-10BiT mice to analyze the temporal IL-10 production by the MDSC subsets in tumor-bearing mice over the course of tumor progression. At two weeks post tumor injection, we observed no IL-10 reporter staining in the blood monocytes (Fig. 3A), and very little reporter in the infiltrating peritoneal CX<sub>3</sub>CR1-positive population. Conversely, we discovered increased IL-10 reporter staining at this time point in the peritoneal CX<sub>3</sub>CR1-negative population (Fig. 3A) compared to staining from naïve peritoneal cells (Fig. 3C). By four weeks post-injection, when mice have developed discernible ascites, we observe the characteristic accumulation of CX<sub>3</sub>CR1-positive cells<sup>9</sup>, and find some IL-10 reporter staining in the blood monocytes as well as substantial reporter staining in the CX<sub>3</sub>CR1-positive and negative peritoneal populations (Fig. 3B). These data indicate that the CX<sub>3</sub>CR1-negative population is an early source of IL-10 in the tumor microenvironment and that the CX<sub>3</sub>CR1-positive MDSC we previously characterized contribute significantly to IL-10 production later in tumor progression.

The IL-10 expression by the CX<sub>3</sub>CR1-negative population is the earliest source of IL-10 that we have detected in the tumor microenvironment. This led us to inquire whether this initial source of IL-10 functions to shape the tumor microenvironment to impact the subsequent tumor progression. We devised a method for temporary in vivo depletion of the IL-10 – expressing cells with the use of the IL-10BiT reporter mice: anti-Thy1.1 antibody specifically depletes the Thy1.1<sup>+</sup> cells, which concomitantly are the in vivo source of IL-10 (Fig. 4A). Based on the temporal window during which the predominant IL-10 expression is by the CX<sub>3</sub>CR1-negative MDSC population (Fig. 3), anti-Thy1.1 antibody was administered to tumor-bearing mice at days 7 and 10 following tumor inoculation. This effectively reduced the IL-10 expressing cells 24 hours after depletion (Fig. 4A) as well as a week later (Fig. 4B); as an internal control, it is worth noting that the CX<sub>3</sub>CR1-positive (and Thy1.1-low) cells were not depleted. Depletion of IL-10 expressing cells modestly reduced CD45-negative cells recovered from the peritoneum of tumor bearing mice a week later, suggesting impaired tumor growth (Fig. 4C). Importantly, the depletion of the Thy1.1<sup>+</sup>/IL-10<sup>+</sup> cells had durable and measurable effects, since this acute depletion of the Thy1.1<sup>+</sup> cells prolonged median survival increased by nearly 3 weeks (Fig. 4D). These data demonstrate a critical functional role for the CX<sub>3</sub>CR1-negative population of MDSCs during early tumor progression and led us to ask whether migration of myeloid cells into the tumor microenvironment prompts the IL-10 expression.

### **Exposure to the tumor microenvironment is sufficient to induce IL-10 production in CX<sub>3</sub>CR1 myeloid subsets**

The ability of IL-10 to enhance its own production suggested to us that the establishment of a tumor-supportive microenvironment early in tumor progression may be important in programming subsequent infiltrating monocytic cells to an IL-10 -producing MDSC phenotype<sup>19, 28</sup>. To better understand the kinetics of IL-10 reporter induction on infiltrating CX<sub>3</sub>CR1-positive cells upon arrival in the tumor microenvironment, we made use of the GR-1 duality of CX<sub>3</sub>CR1-positive cells. As we previously reported, while both the GR-1 -positive and -negative monocytic populations are capable of infiltrating the tumor microenvironment, expression of GR-1 is lost within 48 hours<sup>9</sup>. Thus, CX<sub>3</sub>CR1-positive cells which express GR-1 have recently migrated into the tumor microenvironment. Analyses of the CX<sub>3</sub>CR1-positive cells in the ascites revealed that the GR-1 -positive subset, which represents a minugia of cells in the ascites (consistent with our previous findings), produced very little IL-10 by reporter staining (Figs. 5A, B). However the GR-1<sup>lo</sup> subset was drastically increased in IL-10 reporter staining (Fig. 5B). A direct comparison of the two subsets revealed that the GR-1 -negative population had significantly higher IL-10 reporter staining, which was not present in the GR-1 -negative cells from naïve mice (Fig. 5B). This suggests that tumor-infiltrating GR-1 -positive monocytic cells increase production of IL-10 after migration into the tumor. Consistent with *in vitro* studies by Sinha et al.<sup>28</sup>, these data suggest that IL-10 production was induced in MDSC after infiltration into the tumor microenvironment and exposure to the tumor milieu may enforce IL-10 production and suppressive functions in myeloid cells. From mice with advanced tumors we did detect low levels of IL-10 reporter staining in blood monocytic cells (Fig. 3B). Further analyses indicated that this reporter staining was predominantly on the GR-1 -negative CX<sub>3</sub>CR1 monocytic subset, but it appeared lower than the reporter expression of this subset

in the ascites. This suggests that blood monocytes also increase IL-10 production, however these methods do not allow us to directly determine if the GR-1<sup>-</sup> positive subset increases IL-10 expression upon arrival in the tumor.

As a complimentary method to demonstrate IL-10 induction in CX<sub>3</sub>CR1-positive monocytes upon infiltration into the tumor microenvironment, we adoptively transferred CX<sub>3</sub>CR1-GFP/IL-10BiT dual reporter PBMC by intraperitoneal injection into tumor-bearing mice. Compared to IL-10 reporter staining prior to transfer, 48 hours after being transferred into the tumor microenvironment we detected increased IL-10 reporter staining, with an average of 44 percent of the transferred CX<sub>3</sub>CR1-positive cells inducing IL-10 reporter staining (Fig. 5C). Together, these data indicate that exposure to the tumor microenvironment is sufficient to induce production of IL-10, a marker of suppressive function and phenotype. Thus, the establishment of the tumor microenvironment may represent a critical tipping point in regulating the innate response, which modulates the adaptive response, against an ovarian tumor.

### **The tumor microenvironment alters maturation/differentiation of the CX<sub>3</sub>CR1 cellular populations**

The identification of both phenotypic and functional similarities between the CX<sub>3</sub>CR1-positive and -negative myeloid populations during tumor growth led us to interrogate the origin of the CX<sub>3</sub>CR1-negative population. Likely origins included from the pre-tumor resident peritoneal macrophage population, infiltration and conversion of CX<sub>3</sub>CR1-positive monocytes, or from some other myeloid, blood-derived intermediary between the bone marrow and peritoneum. The observation that the CX<sub>3</sub>CR1-negative population is maintained at a relatively stable frequency within the peritoneum during tumor progression (Fig. 1) despite the dramatic increases in total peritoneal cellularity indicates that this population must be increasing in number either through local proliferation or new recruitment.

A number of studies have investigated the role of CX<sub>3</sub>CR1-positive blood-borne monocytes and their precursor, the macrophage and dendritic cell precursor (MDP), in populating the host myeloid compartment during resting and inflammatory conditions<sup>29,30</sup>. These studies indicate that monocytes and their precursor can give rise to multiple tissue macrophages and myeloid cell subsets, however these studies do not report if these cells can give rise to CX<sub>3</sub>CR1-negative MDSCs. In studies by Fogg et al., the MDP and monocytes, albeit to a dramatically lesser extent, were demonstrated *in vivo* to seed resident splenic macrophage and dendritic cells populations negative for CX<sub>3</sub>CR1. The authors also report that culture of the MDP with GM-CSF yields CD11bCD11c double-positive cells that are negative for CX<sub>3</sub>CR1<sup>29</sup>. We asked if this loss of CX<sub>3</sub>CR1 expression could occur *in vivo* in a peritoneal tumor setting in order to determine if CX<sub>3</sub>CR1-positive precursor cells give rise to the subsequent CX<sub>3</sub>CR1-negative MDSC. To address this question we generated MDP chimeric mice by FACS-sorting GFP-positive MDP that were negative for lineage markers for CD11b, CD11c, CD3, GR-1, NK1.1, and B220 from the bone marrow of CX<sub>3</sub>CR1-GFP mice. These congenically-marked cells were mixed with wild-type bone marrow and used to reconstitute lethally irradiated wild-type mice. This experimental setup allowed us to



identify MDP-derived (CD45.1 congenic) cells in these mice and to assess their expression of CX<sub>3</sub>CR1. We injected MDP chimeric mice with ID8vβ tumors and assessed the ability of these CX<sub>3</sub>CR1-positive precursors to give rise to congenically-marked CX<sub>3</sub>CR1-negative cells in the ascites. We found that after reconstitution and tumor progression, the MDP do indeed give rise to CX<sub>3</sub>CR1-negative cells in the ascites (Fig. 6A), with wild-type tumor-bearing mice stained for CD45.1 as a negative control (Fig. 6A). Interestingly, very few GFP-positive progeny, which we were able to detect immediately after reconstitution (data not shown), were observed in the ascites. However, the time course of this experiment extends beyond the replicative lifespan of MDP, and the initial GFP<sup>+</sup> precursors likely all died or lost expression of CX<sub>3</sub>CR1 upon maturation into the CX<sub>3</sub>CR1-negative subset that we were able to detect. These data indicate that CX<sub>3</sub>CR1-positive precursor cells give rise to CX<sub>3</sub>CR1-negative myeloid populations in vivo.

### **The tumor microenvironment promotes accumulation of CX<sub>3</sub>CR1 -positive MDSC during tumor progression**

While the MDP transfers indicate that CX<sub>3</sub>CR1-positive cells in the bone marrow can give rise to the CX<sub>3</sub>CR1-negative cells in the ascites, whether this occurs before tumor growth through monocyte repopulation of resident cells or at some specific time during tumor progression could not be determined in the chimeric mice. To clarify if this can occur within the tumor microenvironment we performed intratumoral transfers of congenically-marked CX<sub>3</sub>CR1-GFP cells sorted from naïve blood. We discovered a substantial CX<sub>3</sub>CR1-positive population in the ascites as late as five days post transfer (Fig. 6B), which suggests that these cells persist in the tumor microenvironment for extended periods of time as GFP-positive cells. This persistence indicated that during advanced tumor progression infiltrating CX<sub>3</sub>CR1-positive cells maintain CX<sub>3</sub>CR1 expression for long periods of time within the ascites, at a time when the MDP-derived cells in the chimera experiments were already in place and had already undergone CX<sub>3</sub>CR1 down-regulation.

To test this model, we cultured CX<sub>3</sub>CR1-GFP bone marrow in vitro to monitor the stability of the CX<sub>3</sub>CR1-positive cells stimulated with tumor plasma. Normally the CX<sub>3</sub>CR1-positive cells decrease over time in culture or with differentiating stimuli. When cultured in the presence of tumor plasma, we observed a marked increase in the persistence of the CX<sub>3</sub>CR1-positive fraction within the CD11b<sup>+</sup>Ly6G<sup>-</sup> cells in the cultured bone marrow (Fig. 6C), and observed the converse in the percentage of CX<sub>3</sub>CR1-negative cells. This supports the hypothesis that the tumor microenvironment, and specifically, soluble mediators in the ascites enforce the accumulation of the CX<sub>3</sub>CR1-positive myeloid population in the tumor microenvironment.

## **Discussion**

Among recent advancements in the characterization of the mononuclear phagocyte system, CX<sub>3</sub>CR1 has emerged as a valuable marker with both phenotypic and functional importance in normal and pathological myeloid biology. However, despite work from several groups using CX<sub>3</sub>CR1 as a defining marker of mononuclear cells and cell subsets<sup>2, 8, 9, 25</sup>, how CX<sub>3</sub>CR1 expression delineates cellular function remains poorly understood. Here, we have

utilized CX<sub>3</sub>CR1 expression to subset distinct CD11b-positive myeloid cells in the ID8vβ mouse model of ovarian cancer that were previously inseparable by other common myeloid markers. Importantly, our previous focus on CX<sub>3</sub>CR1-positive cells excluded this newly-appreciated suppressive CX<sub>3</sub>CR1-negative fraction within the CD11b<sup>+</sup>CD115<sup>+</sup>Ly6G<sup>-</sup> compartment. Identification of the CX<sub>3</sub>CR1-negative population, and distinguishing it from the CX<sub>3</sub>CR1-positive population (the collective CX<sub>3</sub>CR1<sup>hi</sup> and low populations), within the myeloid compartment in the tumor has allowed us to shed new light on myeloid dynamics and function in regard to IL-10 control of tumor progression.

Two important findings emerge from the temporal dynamics of the CX<sub>3</sub>CR1-negative MDSC population relative to our previous studies on IL-10 functions in the tumor microenvironment. First, these cells may represent an important initiator of a chain reaction of IL-10 signaling in the tumor microenvironment, on which we have shown the function and accumulation of infiltrating MDSC depend<sup>19</sup>. Therefore, the discovery that early IL-10 signaling from the CX<sub>3</sub>CR1-negative population, at a time when the CX<sub>3</sub>CR1-positive population that is present lacks this production, demonstrates a novel and important functional contribution of these cells during early tumor progression and enhances our understanding of myeloid cell dynamics and interactions in the peritoneum. This initiation likely represents a key switch between tumor-recruited myeloid cells capable of initiating and supporting adaptive anti-tumor immunity and tumor-suppressive myeloid cells that accumulate and inhibit adaptive anti-tumor immunity. This premise is further reinforced by our observation that the CX<sub>3</sub>CR1-negative population of MDSCs functionally contribute to tumor progression since depletion of the IL-10<sup>+</sup> CX<sub>3</sub>CR1-negative population significantly and substantially delays tumor progression.

Secondly, we wanted to determine if CX<sub>3</sub>CR1-negative cells could arise from CX<sub>3</sub>CR1-positive precursor cells in the blood or bone marrow. By way of precedent, previous analyses of naïve peritoneal macrophages indicate that the resident macrophage population (since documented to be CX<sub>3</sub>CR1-negative) is seeded almost exclusively by blood monocytes<sup>31</sup>. However, more recent studies that assess the fate of CX<sub>3</sub>CR1-positive monocytes suggest that these monocytes do not give rise to CX<sub>3</sub>CR1-negative cells in the naïve peritoneum within 18 hours<sup>2</sup>. However, both of these studies had an unrelated specific focus and remain incomplete. Here, we demonstrate that CX<sub>3</sub>CR1-positive MDPs are capable of giving rise to CX<sub>3</sub>CR1-negative peritoneal cells *in vivo*. Interestingly, when directly transferred into the tumor, CX<sub>3</sub>CR1-positive monocytes did not undergo this shift quite as strongly. This suggests that monocyte differentiation to CX<sub>3</sub>CR1-negative cells requires an additional *in vivo* stimulus prior to tumor infiltration, the process of transfer impaired this transition, or that CX<sub>3</sub>CR1 negative cells recovered in tumor bearing MDP mice arose prior to or early in tumor progression. The *in vitro* studies carried out here on bone marrow from CX<sub>3</sub>CR1-GFP mice, support the foremost explanation. These experiments indicate that the tumor microenvironment drives the accumulation of CX<sub>3</sub>CR1-positive cells, however whether this is through regulation of CX<sub>3</sub>CR1 gene expression or by increasing the survival of these cells *in vitro* and *in vivo* is unclear.

In summary, the regulation of anti-tumor immunity by myeloid populations within the tumor is emerging as an important aspect of tumor progression. Data indicate that these cells are

involved in tumor escape from immune pressure, metastasis of tumor cells, and importantly, contribute significantly to blocking immunotherapeutic strategies. Thus, understanding the networks controlling the development, accumulation and function of myeloid cells is critical to advancing our understanding and potential interventions in disease. Here we have presented work focused on utilizing the CX<sub>3</sub>CR1 axis to improve our understanding of myeloid cells dynamics, the emergence of MDSC within the tumor microenvironment, the initiation of the suppressive IL-10 network, and control of the tumor microenvironment. These studies provide insight into progressive immune processes, as well as identify new targets and strategies to therapeutically intervene in tumors and other immune maladies.

## Supplementary Material

Refer to Web version on PubMed Central for supplementary material.

## Acknowledgments

The authors thank Drs. Katelyn Byrne, Mary Jo Turk, and Alan Howe for helpful reagents and discussions. This research was supported by NIH R01 AI067405, American Cancer Society grant RSG-10-229-01-LIB, and a UMass/Dartmouth/UVM Cancer Centers Collaborative Research Program Grant (Brent Berwin) and T32 GM08704 and T32 AI007363 (Kevin M. Hart).

## Abbreviations Page

|             |                                     |
|-------------|-------------------------------------|
| <b>FACS</b> | Fluorescence-activated Cell Sorting |
| <b>GFP</b>  | Green Fluorescent Protein           |
| <b>LPS</b>  | Lipopolysaccharide                  |
| <b>MDSC</b> | Myeloid Derived Suppressor cell     |
| <b>MDP</b>  | Macrophage Dendritic cell Precursor |
| <b>MFI</b>  | Mean Fluorescence Intensity         |
| <b>PBMC</b> | Peripheral Blood Mononuclear Cells  |
| <b>PBS</b>  | Phosphate Buffered Solution         |

## References

1. Geissmann F, Auffray C, Palframan R, Wirrig C, Ciocca A, Campisi L, et al. Blood monocytes: distinct subsets, how they relate to dendritic cells, and their possible roles in the regulation of T-cell responses. *Immunol Cell Biol.* 2008; 86:398–408. [PubMed: 18392044]
2. Geissmann F, Jung S, Littman DR. Blood monocytes consist of two principal subsets with distinct migratory properties. *Immunity.* 2003; 19:71–82. [PubMed: 12871640]
3. Kayama H, Ueda Y, Sawa Y, Jeon SG, Ma JS, Okumura R, et al. Intestinal CX<sub>3</sub>C chemokine receptor 1(high) (CX<sub>3</sub>CR1(high)) myeloid cells prevent T-cell-dependent colitis. *Proc Natl Acad Sci U S A.* 2012; 109:5010–5. [PubMed: 22403066]
4. Rivollier A, He J, Kole A, Valatas V, Kelsall BL. Inflammation switches the differentiation program of Ly6Chi monocytes from antiinflammatory macrophages to inflammatory dendritic cells in the colon. *J Exp Med.* 2012; 209:139–55. [PubMed: 22231304]

5. Clover AJ, Kumar AH, Caplice NM. Deficiency of CX3CR1 delays burn wound healing and is associated with reduced myeloid cell recruitment and decreased sub-dermal angiogenesis. *Burns*. 2011; 37:1386–93. [PubMed: 21924836]
6. Bonduelle O, Duffy D, Verrier B, Combadiere C, Combadiere B. Cutting edge: Protective effect of CX3CR1+ dendritic cells in a vaccinia virus pulmonary infection model. *J Immunol*. 2012; 188:952–6. [PubMed: 22219332]
7. Donnelly DJ, Longbrake EE, Shawler TM, Kigerl KA, Lai W, Tovar CA, et al. Deficient CX3CR1 signaling promotes recovery after mouse spinal cord injury by limiting the recruitment and activation of Ly6Clo/iNOS+ macrophages. *J Neurosci*. 2011; 31:9910–22. [PubMed: 21734283]
8. Karlmark KR, Zimmermann HW, Roderburg C, Gassler N, Wasmuth HE, Luedde T, et al. The fractalkine receptor CX(3)CR1 protects against liver fibrosis by controlling differentiation and survival of infiltrating hepatic monocytes. *Hepatology*. 2010; 52:1769–82. [PubMed: 21038415]
9. Hart KM, Bak SP, Alonso A, Berwin B. Phenotypic and functional delineation of murine CX(3)CR1 monocyte-derived cells in ovarian cancer. *Neoplasia*. 2009; 11:564–73. [PubMed: 19484145]
10. Shah R, Hinkle CC, Ferguson JF, Mehta NN, Li M, Qu L, et al. Fractalkine is a novel human adipochemokine associated with type 2 diabetes. *Diabetes*. 2011; 60:1512–8. [PubMed: 21525510]
11. Zeyda M, Gollinger K, Kriehuber E, Kiefer FW, Neuhofer A, Stulnig TM. Newly identified adipose tissue macrophage populations in obesity with distinct chemokine and chemokine receptor expression. *Int J Obes (Lond)*. 2010; 34:1684–94. [PubMed: 20514049]
12. Ishida Y, Hayashi T, Goto T, Kimura A, Akimoto S, Mukaida N, et al. Essential involvement of CX3CR1-mediated signals in the bactericidal host defense during septic peritonitis. *J Immunol*. 2008; 181:4208–18. [PubMed: 18768878]
13. Ishida Y, Gao JL, Murphy PM. Chemokine receptor CX3CR1 mediates skin wound healing by promoting macrophage and fibroblast accumulation and function. *J Immunol*. 2008; 180:569–79. [PubMed: 18097059]
14. Tighe RM, Li Z, Potts EN, Frush S, Liu N, Gunn MD, et al. Ozone inhalation promotes CX3CR1-dependent maturation of resident lung macrophages that limit oxidative stress and inflammation. *J Immunol*. 2011; 187:4800–8. [PubMed: 21930959]
15. Bak SP, Alonso A, Turk MJ, Berwin B. Murine ovarian cancer vascular leukocytes require arginase-I activity for T cell suppression. *Mol Immunol*. 2008; 46:258–68. [PubMed: 18824264]
16. Bak SP, Walters JJ, Takeya M, Conejo-Garcia JR, Berwin BL. Scavenger receptor-A-targeted leukocyte depletion inhibits peritoneal ovarian tumor progression. *Cancer Res*. 2007; 67:4783–9. [PubMed: 17510407]
17. Huarte E, Cubillos-Ruiz JR, Nesbeth YC, Scarlett UK, Martinez DG, Buckanovich RJ, et al. Depletion of dendritic cells delays ovarian cancer progression by boosting antitumor immunity. *Cancer Res*. 2008; 68:7684–91. [PubMed: 18768667]
18. Scarlett UK, Cubillos-Ruiz JR, Nesbeth YC, Martinez DG, Engle X, Gewirtz AT, et al. In situ stimulation of CD40 and Toll-like receptor 3 transforms ovarian cancer-infiltrating dendritic cells from immunosuppressive to immunostimulatory cells. *Cancer Res*. 2009; 69:7329–37. [PubMed: 19738057]
19. Hart KM, Byrne KT, Molloy MJ, Usherwood EM, Berwin B. IL-10 immunomodulation of myeloid cells regulates a murine model of ovarian cancer. *Front Immunol*. 2011; 2:29. [PubMed: 22566819]
20. Hagemann T, Wilson J, Burke F, Kulbe H, Li NF, Pluddemann A, et al. Ovarian cancer cells polarize macrophages toward a tumor-associated phenotype. *J Immunol*. 2006; 176:5023–32. [PubMed: 16585599]
21. Hagemann T, Lawrence T, McNeish I, Charles KA, Kulbe H, Thompson RG, et al. “Re-educating” tumor-associated macrophages by targeting NF-kappaB. *J Exp Med*. 2008; 205:1261–8. [PubMed: 18490490]
22. Mustea A, Konsgen D, Braicu EI, Pirvulescu C, Sun P, Sofroni D, et al. Expression of IL-10 in patients with ovarian carcinoma. *Anticancer Res*. 2006; 26:1715–8. [PubMed: 16617566]
23. Mustea A, Braicu EI, Koensgen D, Yuan S, Sun PM, Stamatian F, et al. Monitoring of IL-10 in the serum of patients with advanced ovarian cancer: results from a prospective pilot-study. *Cytokine*. 2009; 45:8–11. [PubMed: 19071030]

24. Nowak M, Glowacka E, Szpakowski M, Szylo K, Malinowski A, Kulig A, et al. Proinflammatory and immunosuppressive serum, ascites and cyst fluid cytokines in patients with early and advanced ovarian cancer and benign ovarian tumors. *Neuro Endocrinol Lett.* 2010; 31:375–83. [PubMed: 20588232]
25. Jung S, Aliberti J, Graemmel P, Sunshine MJ, Kreutzberg GW, Sher A, et al. Analysis of fractalkine receptor CX(3)CR1 function by targeted deletion and green fluorescent protein reporter gene insertion. *Mol Cell Biol.* 2000; 20:4106–14. [PubMed: 10805752]
26. Maynard CL, Harrington LE, Janowski KM, Oliver JR, Zindl CL, Rudensky AY, et al. Regulatory T cells expressing interleukin 10 develop from Foxp3+ and Foxp3– precursor cells in the absence of interleukin 10. *Nat Immunol.* 2007; 8:931–41. [PubMed: 17694059]
27. Conejo-Garcia JR, Benencia F, Courreges MC, Kang E, Mohamed-Hadley A, Buckanovich RJ, et al. Tumor-infiltrating dendritic cell precursors recruited by a beta-defensin contribute to vasculogenesis under the influence of Vegf-A. *Nat Med.* 2004; 10:950–8. [PubMed: 15334073]
28. Sinha P, Clements VK, Bunt SK, Albelda SM, Ostrand-Rosenberg S. Cross-talk between myeloid-derived suppressor cells and macrophages subverts tumor immunity toward a type 2 response. *J Immunol.* 2007; 179:977–83. [PubMed: 17617589]
29. Fogg DK, Sibon C, Miled C, Jung S, Aucouturier P, Littman DR, et al. A clonogenic bone marrow progenitor specific for macrophages and dendritic cells. *Science.* 2006; 311:83–7. [PubMed: 16322423]
30. Auffray C, Fogg DK, Narni-Mancinelli E, Senechal B, Trouillet C, Saederup N, et al. CX3CR1+ CD115+ CD135+ common macrophage/DC precursors and the role of CX3CR1 in their response to inflammation. *J Exp Med.* 2009; 206:595–606. [PubMed: 19273628]
31. Murch AR, Grounds MD, Papadimitriou JM. Improved chimaeric mouse model confirms that resident peritoneal macrophages are derived solely from bone marrow precursors. *J Pathol.* 1984; 144:81–7. [PubMed: 6491835]

**Summary sentence**

Identification of ovarian tumor-infiltrating CX<sub>3</sub>CR1-negative cells as myeloid suppressor cells and as a cellular subset with physiological and functional specificity.

Author Manuscript

Author Manuscript

Author Manuscript

Author Manuscript

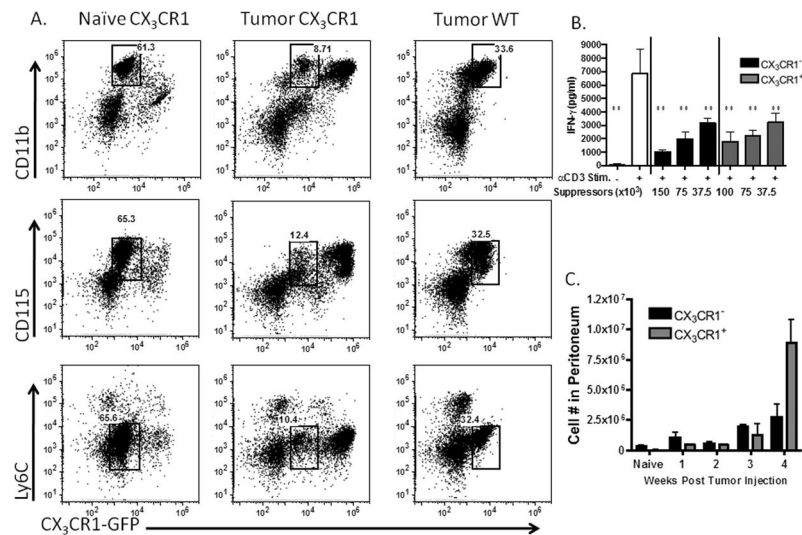


**Figure 1. CX<sub>3</sub>CR1 expression delineates two distinct tumor-infiltrating myeloid populations that potently suppress T cell reactivity**

(A) Representative flow plots from naïve peritoneal lavages and ascites of tumor-bearing CX<sub>3</sub>CR1-GFP mice compared to ascites from wild type tumor-bearing mice. Stained for CD115, CD11b and Ly-6C. Gates shown identify the CX<sub>3</sub>CR1-negative macrophage population. (B) CX<sub>3</sub>CR1<sup>-</sup> and -positive cell subsets were sorted by flow cytometry and titrated into a mixed splenocyte reaction stimulated with anti-CD3 to test for suppressive capacity, with averages and standard deviation shown, results represent three independent experiments. (C) Total numbers of CX<sub>3</sub>CR1<sup>-</sup> and -positive cells within the peritoneum of naïve mice, and tumor-bearing mice over the course of tumor progression (n=3 mice). \*\*p<.01 in comparison to stimulated (open bar) cells. Standard deviations shown.

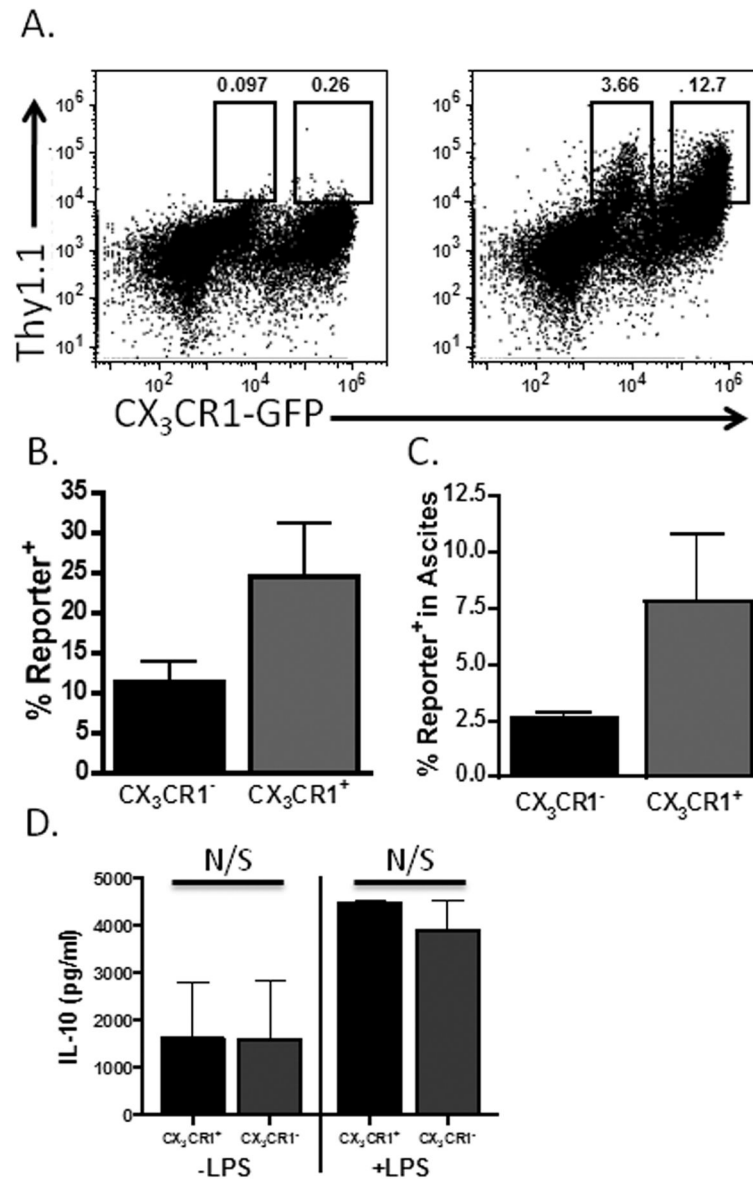


**Figure 2. CX<sub>3</sub>CR1 expression delineates two distinct IL-10 producing populations in the ascites of ovarian tumor-bearing mice**

(A) The ascites of ID8v $\beta$  tumor-bearing CX<sub>3</sub>CR1-GFP/IL-10BiT mice (right) was analyzed for IL-10 expression (Thy1.1 reporter staining) on the CX<sub>3</sub>CR1 MDSC population compared to CX<sub>3</sub>CR1-GFP mice not carrying the BiT reporter transgene (left) (representative data from 10 mice). (B) Quantification of the percentage of reporter positive cells within the pre-gated populations from CX<sub>3</sub>CR1-GFP/IL-10BiT mice. (C) The percentage composition of reporter positive cells from the CX<sub>3</sub>CR1-positive and negative fractions within the ascites (n=3 mice). (D) Sorted CX<sub>3</sub>CR1-positive and -negative cell subsets from tumor-bearing mice were cultured with or without LPS stimulation for 72 hours, and the media subsequently assessed by ELISA for IL-10 (IL-10 production normalized to 10<sup>5</sup> cells). N/S not significant (p > .05), standard deviations shown.



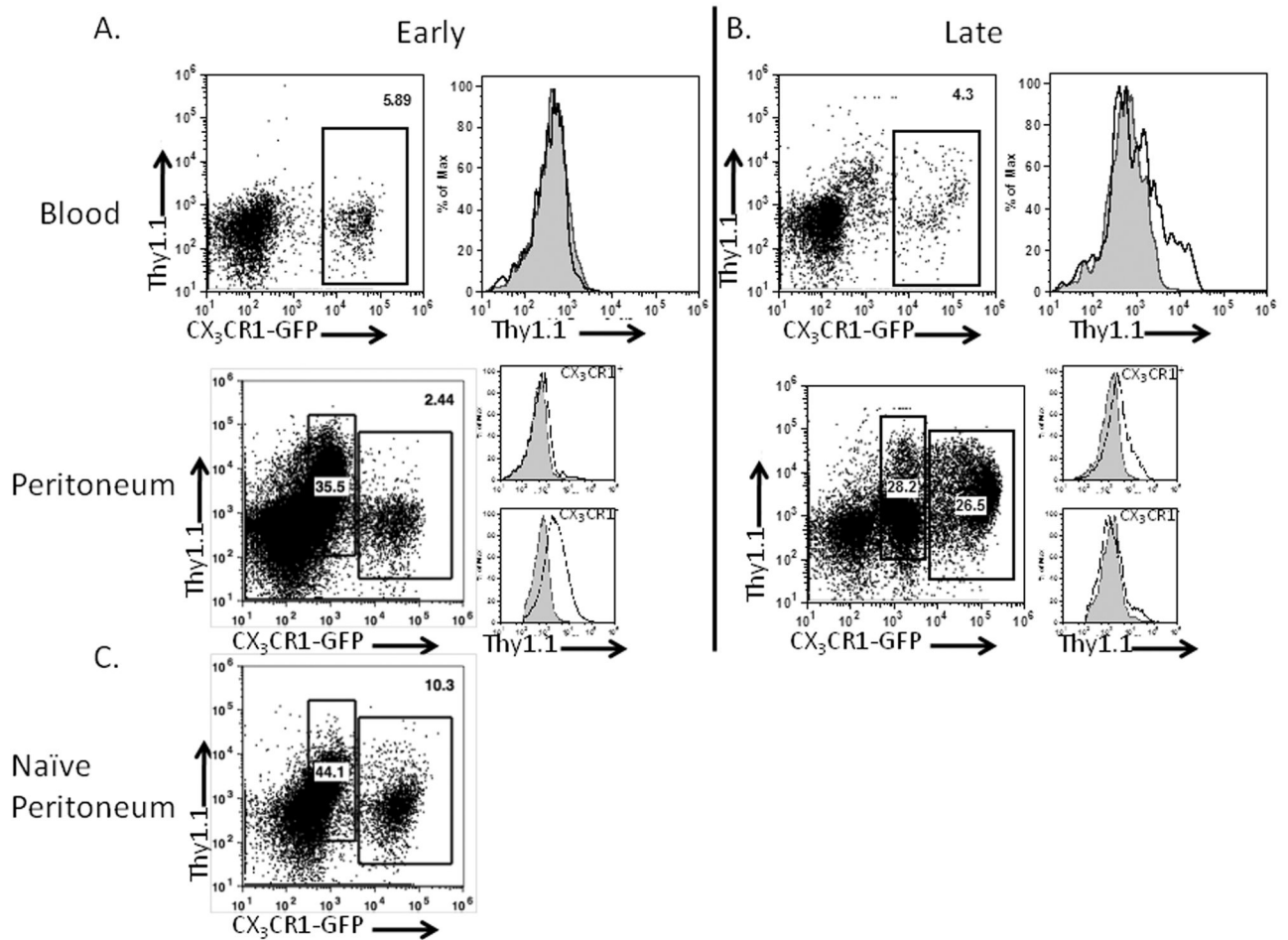


**Figure 3. IL-10 production is initiated in CX<sub>3</sub>CR1-negative MDSCs and subsequently is detected in CX<sub>3</sub>CR1-positive MDSCs in tumor-bearing mice**

Blood and peritoneal samples from 2 (A) and 4-week (B) ID8v $\beta$  tumor-bearing mice were assessed for IL-10 reporter staining. Plots of CX<sub>3</sub>CR1-GFP/IL-10BiT reporter staining and histograms indicate reporter staining in gated populations in CX<sub>3</sub>CR1-GFP/IL-10BiT mice (black) in comparison to CX<sub>3</sub>CR1-GFP control mice (gray, filled) representative of results from 5 mice. (C) Staining from the peritoneum of naïve CX<sub>3</sub>CR1-GFP/IL-10BiT reporter.

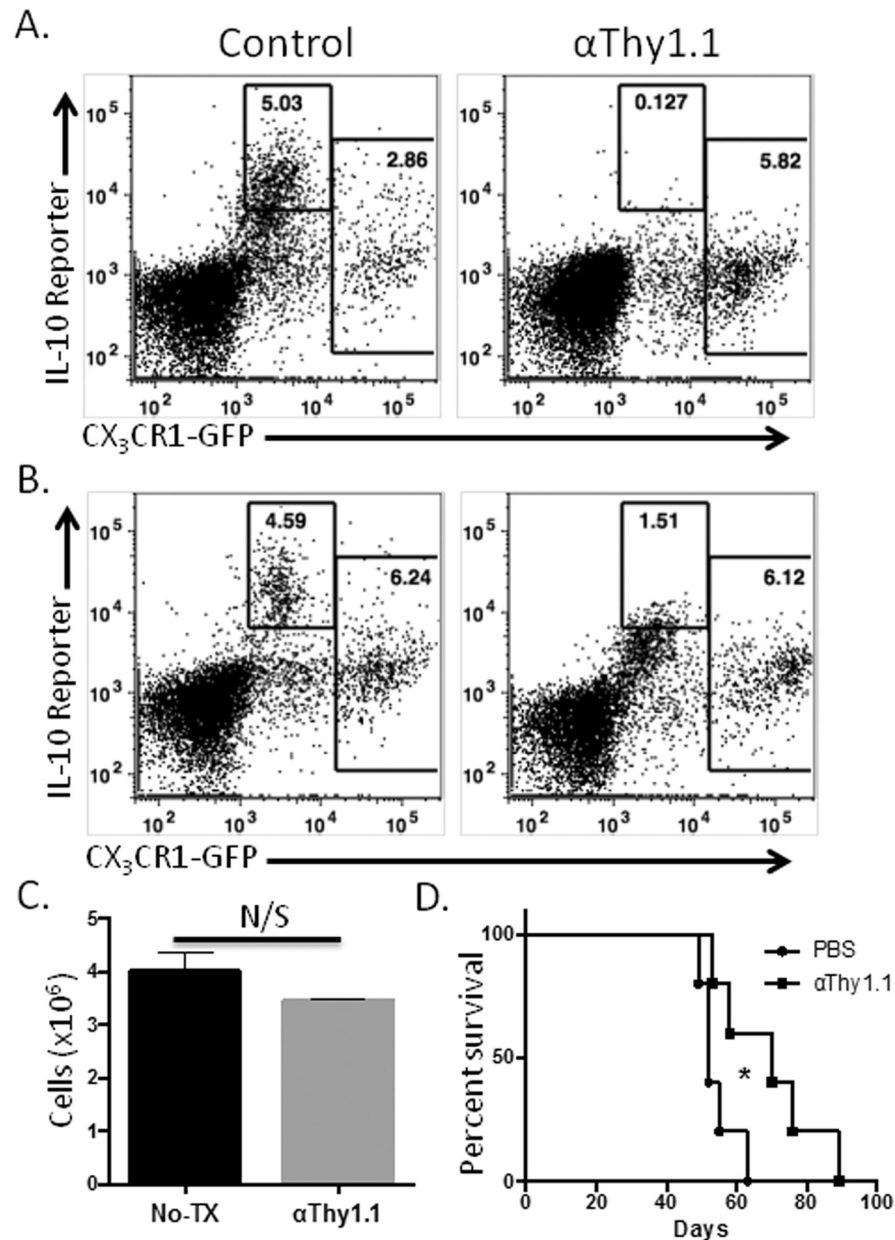


**Figure 4. Depletion of early IL-10 –expressing MDSCs inhibits tumor progression**  
 ID8v $\beta$  tumor-bearing IL-10BiT reporter mice were injected with 500  $\mu$ g of anti-Thy1.1 antibody on days 7 and 10 following tumor inoculation to deplete IL-10 –expressing, Thy1.1<sup>+</sup>, cells. This lowered the CX<sub>3</sub>CR1-negative IL-10 reporter positive staining 48 hours after antibody depletion (Gate set using non-BiT CX<sub>3</sub>CR1 control mouse) (A). (B) Thy1.1 IL-10 reporter staining one week after depletion. (C) CD45-negative peritoneal cells recovered one week after depletion. (D) Thy1.1-mediated depletion of the IL-10 –expressing MDSC on days 7 and 10 in ID8v $\beta$  tumor-bearing IL-10BiT reporter mice results in prolonged survival (Kaplan Meier analysis; n=5 mice, 2 independent experiments; \*p<.05). N/S not significant (p .05).

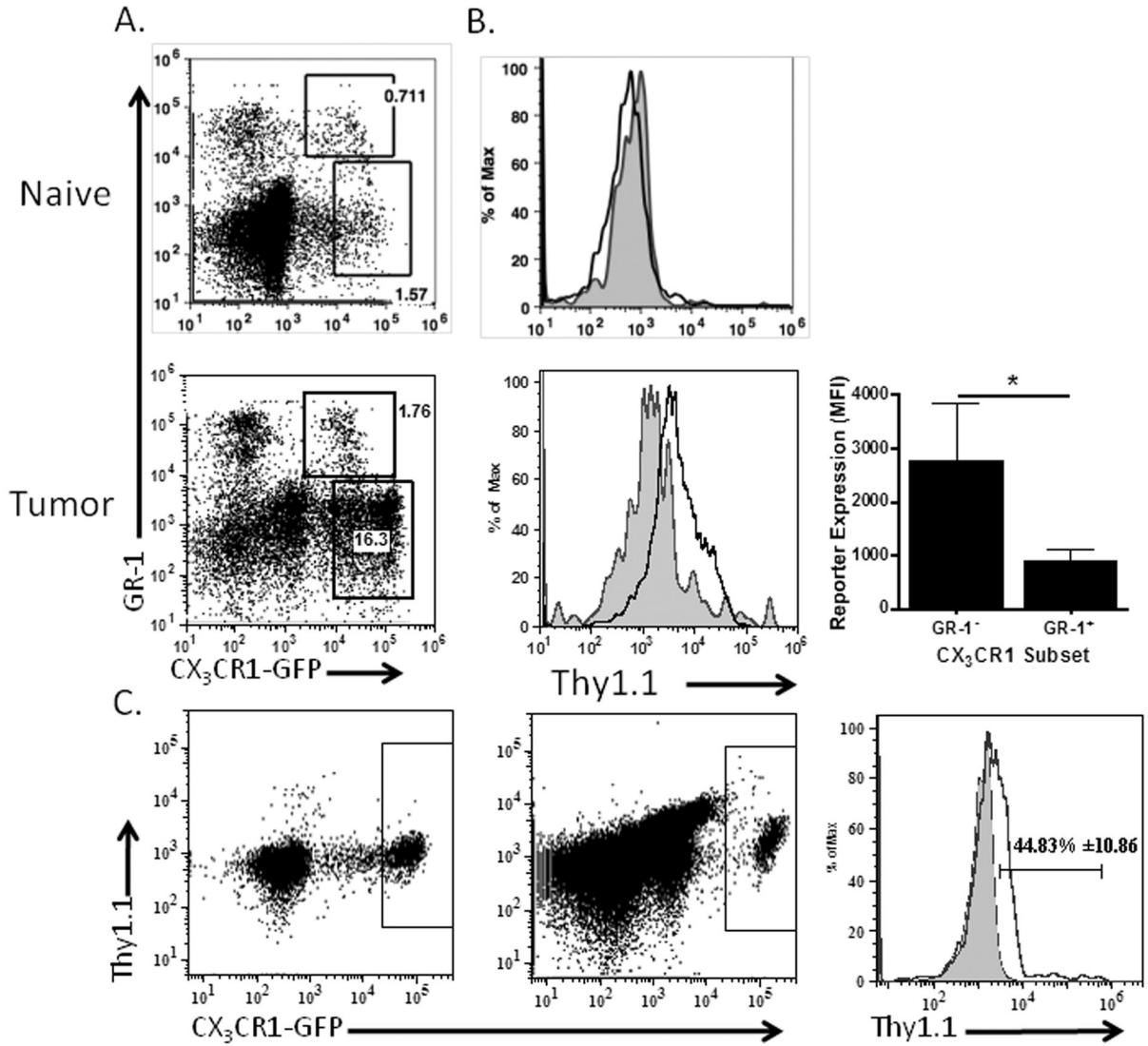


**Figure 5. IL-10 reporter is induced in infiltrating CX<sub>3</sub>CR1-positive monocytic MDSC**  
 (A) GR-1 positive and negative CX<sub>3</sub>CR1-positive cells in the naïve peritoneum, or ascites of tumor-bearing CX<sub>3</sub>CR1-GFP/IL-10BiT mice were analyzed for IL-10 reporter staining. Plot shows GR-1 positive and negative gates. (B) Histogram indicates reporter staining on gated populations from CX<sub>3</sub>CR1-GFP/IL-10BiT mice showing GR-1 negative (black) compared to GR-1 positive (gray, filled) with quantification of IL-10 reporter staining from gated populations (panel A) by MFI. (C) Plots demonstrating reporter staining on CX<sub>3</sub>CR1-GFP positive cells before (left dot plot) and after transfer (right dot plot) of PBMC from CX<sub>3</sub>CR1-GFP/IL-10BiT mice i.p. into a wild-type tumor bearing recipient, with comparative histogram of IL-10 reporter staining pre (gray filled) and post (black) transfer showing percentage positive for reporter staining with standard deviation. n=3 independent experiments, 3 mice. Statistical significance (\**p* < 0.05) and standard deviations shown.

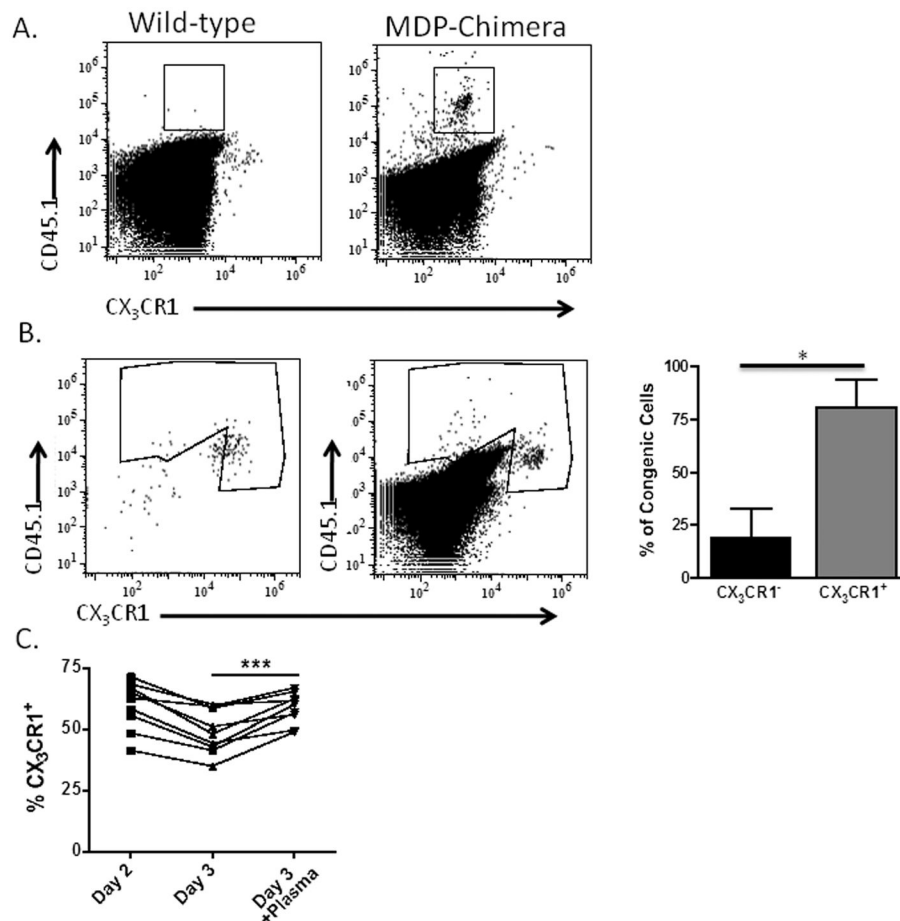


**Figure 6. Tumor-infiltrating myeloid cells generated from the macrophage/dendritic cell precursor (MDP) lose CX<sub>3</sub>CR1 expression, but tumor-transferred monocytes maintain CX<sub>3</sub>CR1 expression**

(A) Ascites from ID8vβ tumor-bearing wild-type mouse (left) and MDP-reconstituted (right) mouse were assessed for CX<sub>3</sub>CR1-negative (gate shown), congenically-marked cells results representative of 2 independent experiments, 6 mice. (B) Sorted CX<sub>3</sub>CR1-GFP positive cells from naïve blood (left plot) were adoptively transferred into the peritoneum of tumor bearing wild-type mice and assessed for GFP expression 4 days post-transfer (right plot) with quantification of CX<sub>3</sub>CR1 positive and negative subsets in the congenic gate with standard deviation (n=4, 4 mice). (C) Percentages of CX<sub>3</sub>CR1-positive cells pre-gated for CD11b<sup>+</sup>Ly6G<sup>-</sup> in bone marrow cultured overnight, and with or without addition of tumor ascites plasma for an additional 24 hours (n=9, 3 independent experiments). Statistical significance (\*\*\*)*p* < 0.001 and \*)*p* < .05 and standard deviations shown.